Theses/Capstones/Creative Projects   University Honors Program

5-2024

Characterizing the role of PA5189 of Pseudomonas aeruginosa in deletion and overexpression mutants

Seh Na Mellick
smellick@unomaha.edu

Recommended Citation

UNO LIBRARIES
LIBRARY.UNOMAHA.EDU

Characterizing the role of PA5189 of *Pseudomonas aeruginosa* in deletion and overexpression mutants

Honors Thesis

University of Nebraska-Omaha

Seh Na Mellick

January 2024

Donald Rowen, PhD

TABLE OF CONTENTS

Abstract

In the context of rising multidrug resistance in biofilm-forming pathogens like *Pseudomonas aeruginosa*, this study investigates the role of the understudied transcription factor PA5189 in antibiotic resistance and biofilm formation. PA5189 deletion and overexpression mutants were created in a parent *P. aeruginosa* strain using pEX18Tc-based recombinant suicide vectors, with genotypic verification of putative triparental conjugants achieved through restriction digestion and PCR. The study revealed that PA5189 overexpression significantly increases resistance to commonly used broad spectrum antibiotics such as ciprofloxacin and imipenem. Additionally, differential expression of PA5189 was found to notably affect biofilm formation, with variations contingent on the nutrient composition and salt content of the growth medium. These findings underscore the role of PA5189 in the adaptive mechanisms of *P. aeruginosa*, contributing to our understanding of the genetic regulation of pathogenicity and offering new insights for targeted antibacterial strategies in the perpetual fight against drug-resistant infections.

List of Tables and Figures

Introduction

The escalating prevalence of antimicrobial resistance in pathogenic bacteria presents a critical challenge to modern medicine, thus necessitating the exploration and development of novel alternatives to conventional antibiotic therapies. Traditional antibiotics, primarily designed to eradicate or inhibit bacterial growth, play an instrumental role in reducing morbidity and mortality associated with bacterial infections [5-6, 30-31]. However, their efficacy is increasingly undermined by factors including inappropriate dosage, differential treatment effectiveness, and the natural evolutionary processes in pathogens. These same factors have also contributed to the emergence and propagation of antibiotic-resistant strains [30].

Additionally, the widespread usage of multidrug treatments in contemporary healthcare and agricultural environments further exacerbates this issue [1-6, 32-33]. In the face of escalating antibiotic consumption and bacterial drug resistance, the current practices in biomedicine and agribusiness contribute to global scenario where antibiotic resistance has become palpably fixed within communities, thus posing significant threats to public health and raising ethical issues related to social justice [30-31, 33]. This situation underscores the critical need to reevaluate our reliance on traditional antibiotic therapies and highlights the urgency of developing new therapeutic alternatives and adjuncts to existing treatments.

Moreover, this challenge is further amplified by the proliferation and pathogenesis of multidrug-resistant (MDR) bacterial strains, which complicates the landscape of infectious disease management [2, 7-8]. These strains, endowed with enhanced pathogenicity, present a formidable and resource-intensive challenge to global public health by adversely impacting mortality and morbidity indices while simultaneously exerting significant financial strains on healthcare systems. The development of multidrug resistance in response to overconsumption of antibiotics is often a consequence of genetic mutations and the acquisition of resistance

genes, thus contributing to the intrinsic virulence of pathogenic strains of bacteria [2]. The rise of MDR strains necessitates a deeper understanding of the genetic mechanisms underlying bacterial survival mechanisms, thereby informing the development of targeted therapies that can effectively counteract these survival strategies.

A notable adaptive strategy employed by bacteria to increase pathogenicity is the formation of biofilms, a process characterized by distinct, highly regulated adaptation mechanisms. Biofilms are complex aggregates of multicellular communities often attached to a surface and embedded in a matrix of extracellular polymeric substances. This matrix provides structural stability, protection, and communal proximity to other bacterial cells [12-14]. Regulated by quorum sensing, the biofilm formation process leverages communication between cells, thus enabling individual bacterial cells within localized microcommunities to gauge proximal population densities as well as communicate and coordinate their behavior in response to intracellular and intercellular signalling [21-23]. As such, biofilms are notoriously resilient due to their heterogeneity, surface adhesion capabilities, and their role in facilitating the acquisition of antibiotic resistance genes [25, 32]. These adaptations, modulated by transcriptomic reorganization, facilitate the transition from planktonic to multicellular biofilm states, enabling bacteria to withstand environmental stressors and evade antimicrobial interventions [17-25]. The clinical implications of biofilm formation are profound, particularly in the treatment of lung, wound, and indwelling catheter infections [26], thus underscoring the importance of unravelling the genetic regulatory mechanisms that drive pathogenic functions like drug resistance and biofilm formation.

Pseudomonas aeruginosa, an opportunistic Gram-negative bacterial pathogen, epitomizes the challenges posed by antibiotic resistant, biofilm-forming bacteria. Accounting for nearly 10% of bacterial infections in clinical settings [37-38], *P. aeruginosa* is characterized by a highly adaptable genome and an intrinsic resistance to many classes of

commonly used antibiotics [1-4]. Identified as an ESKAPE pathogen by the World Health Organization, it signifies a category of bacteria that are extensively drug-resistant and for which novel therapeutic approaches are urgently needed [39]. The ability of *P. aeruginosa* to modify its transcriptome and form robust biofilms assists it in the evasion of therapeutic interventions and host immune responses [40-41]. As such, deciphering the regulatory mechanisms of genes in *P. aeruginosa* involved in drug resistance and biofilm formation is vital for understanding its adaptive responses and identifying potential targets for new antimicrobial treatments.

In the search for novel antimicrobial agents, a key focus is unravelling how *P. aeruginosa* modulates cellular processes that contribute to its virulence. Central to this understanding are transcription factors (TFs), which regulate gene expression, thereby influencing various cellular processes. Investigating TFs and their binding sites (TFBS) can provide insights into the complex genetic regulation and interactions, illuminating how *P. aeruginosa* regulates its pathogenicity [43]. One such gene in *P. aeruginosa,* PA5189, is a TFBS and probable transcription factor which has garnered interest due to its proposed relevance in virulence pathways. Although PA5189 is relatively unstudied, preliminary research has suggested that it acts as a direct repressor of the *BsrA* transcription factor and is also known to bind to the disease-relevant *mvfR* transcription factor, thereby placing it within a complex transcriptional regulatory network [44]. *BsrA* is known to play a role in inhibiting biofilm synthesis and influencing the expression of genes crucial for cellular metabolism, transport, and formation of surface appendages [44]. As such, elucidating how PA5189 influences these cellular processes could advance our understanding of the networks underlying virulence pathways which assist *P. aeruginosa* in evading antibacterial treatments.

The Rowen lab has isolated a mutant strain of *P. aeruginosa*, F2, which shows altered sensitivity to broad-spectrum antibiotics such as polymyxin B, colistin, tobramycin,

ciprofloxacin, ceftriaxone, and imipenem. This mutation caused overexpression of the

PA5189 gene, as well as a nonsynonymous single-nucleotide polymorphism changing a

single base pair in the *pmrB* gene [29]. Given the virulence of F2 as well as previous findings

implicating PA5189 in disease-relevant genetic pathways, developing *P. aeruginosa* strains

containing isolated PA5189 mutations can contribute to characterizing the impact of PA5189

on drug resistance and biofilm formation in *P. aeruginosa*. Since isolating F2, the Rowen lab

has generated a strain of *P. aeruginosa*, PA01-428, exhibiting wild-type *pmrB* and

upregulation of PA5189 [29]. In this study, we aim to generate a ΔPA5189 mutant

experiencing knockout of PA5189 and subsequently examine drug sensitivity and biofilm

formation to contrast the effects of differential expression of PA5189 on virulence.

Methods

Media and strain preparation

In this study, a variety of bacterial strains were employed as detailed in Table 1. These

strains were propagated overnight in different growth media, tailored to the specific

requirements of each experiment. For routine cultivation, the strains were grown overnight in

nutrient-rich LB Miller broth, composed of 10 g/L tryptone, 5 g/L yeast extract, and 5 g/L

NaCl with the pH adjusted to 7.0. For cloning experiments, Tryptic Soy broth was used,

which comprised of 17.0 g/L casein peptone (pancreatic), 3.0 g/L soya peptone (papain

digest), 5.0 g/L NaCl, 2.5 g/L dipotassium hydrogen phosphate, and 2.5 g/L glucose, with a

pH of 7.3. Additionally, cation-adjusted Mueller-Hinton (CAMH) broth, containing 3.0 g/L

beef extract, 17.5 g/L acid hydrolysate of casein, 1.5 g/L starch, 20 mg/L $CaCl_2$, and 11 mg/L

$MgCl_2$, was utilized for growth assays.

For short-term storage, the strains were maintained on LB-agar medium, which is LB

broth supplemented with 15 g/L agar. Following inoculation, the strains were incubated

overnight under aerobic conditions at 37 °C. Plasmid selection in *Escherichia coli* (*E. coli*)

was conducted by supplementing the growth media with antibiotics, specifically 3 µg/mL

tetracycline, 50 µg/mL kanamycin, or 25 µg/mL gentamicin. Concurrently, *Pseudomonas*

aeruginosa (*P. aeruginosa*) was grown overnight in LB and CAMH broth under similar

conditions. For *P. aeruginosa*, short-term storage involved cultivation on Pseudomonas

Isolation Agar (PIA-agar), comprising 20.0 g/L enzymatic digest of gelatin, 11.4 g/L $MgCl_2$,

10.0 g/L K_2SO_4, 0.025 g/L irgasan, 13.6 g/L agar, and 25.2 g/L glycerol. Plasmid selection in

P. aeruginosa was achieved by supplementing PIA-agar growth media with 100-200 µg/mL

tetracycline or 200 µg/mL gentamicin.

For use in growth and drug assays, strains were propagated in both liquid LB and

CAMHB media using overnight incubation at 37 °C with constant agitation. Subsequent to a

100-fold dilution in fresh media, the subcultured strains were incubated under the same

conditions. The growth progression was monitored by measuring the optical densities at 600

nm (OD_{600}), with particular attention to capturing the logarithmic phase of growth, indicated

by OD_{600} values between approximately 0.1 and 0.6 OD_{600}/mL.

In the preparation of competent *E. coli* cells, a critical step for transformation

experiments, overnight cultures were inoculated in LB Miller broth and incubated under

aerobic conditions at 37 °C. A 100-fold dilution of the overnight culture was made in fresh

media, and the subcultured strains were incubated similarly. Monitoring the growth

conditions via spectrophotometer as described previously, the strains were grown until

achieving approximately 0.4 OD_{600}/mL, indicating log-phase growth. Cells were then treated

with a solution containing 60mM $CaCl_2$ and 10mM PIPES buffer (pH 7.0). Post-treatment,

the cells were resuspended in 15% glycerol, rapidly cooled using dry ice, and subsequently

stored at -80 °C for long-term preservation.

For use in triparental conjugation experiments, *P. aeruginosa* strains were initially

cultivated overnight in LB broth. Following this, the strains were incubated at 42 °C with

agitation to eliminate restriction enzyme star activity in the recipient cells. This approach was designed to optimize the transfer of genetic material into *P. aeruginosa*, thereby facilitating the conjugation process.

Recombinant DNA methods

In this study, sequence information pertinent to *Pseudomonas aeruginosa* was acquired from the *Pseudomonas* Genome Database (www.pseudomonas.com). Our approach employed polymerase chain reaction (PCR) to generate specific inserts for both knockout and overexpression studies targeting the PA5189 gene (Table 1). The PCR amplifications of *P. aeruginosa* genomic DNA were conducted using a standardized reaction mixture. This recipe comprised of approximately 150-200 ng of PA01 genomic DNA, 200 µM of each deoxynucleotide triphosphate (dNTP) provided by Fisher Scientific, 1X Q5 buffer, 1X Q5 GC enhancer to facilitate the amplification of GC-rich regions, and 10 µM of both forward and reverse primers. Additionally, the reaction mixture contained 50 mM $MgCl_2$ to stabilize the DNA polymerase and 0.5 U/µL Q5 high-fidelity DNA polymerase (New England Biolabs), optimized for robust and accurate amplification.

The resultant amplicons generated from PCR were then subjected to purification using the GeneJET PCR Purification Kit (Thermo Scientific™) to ensure the removal of unincorporated primers and dNTPs. Concurrently, plasmids used in these studies were extracted and purified with the GeneJET Plasmid Miniprep Kit (Thermo Scientific™). Both plasmids and PCR products, typically at concentrations of 30-50 ng/µL, were digested for 60 minutes at 37 °C using 0.05 U/µL Fast Digest enzymes (Thermo Scientific™) along with 1X FD buffer (Thermo Scientific™). This step was crucial for preparing the DNA fragments for subsequent cloning procedures.

Post-digestion, the products were analyzed through agarose gel electrophoresis for assessment of digestion efficiency. The gels were prepared with 0.7-1% agarose and stained

with 0.05 µg/mL ethidium bromide for DNA visualization. DNA fragments of interest were extracted from the gel using the ThermoScientific™ Silica Bead DNA Gel Extraction Kit.

Ligation reactions were conducted by combining approximately 45 fmol of the digested PCR product and 15 fmol of the digested plasmid DNA. The reactions also included 1X ligation buffer, and 0.5-1 U/µL T4 ligase (ThermoScientific™). These ligations were incubated overnight at 16 °C to facilitate the efficient joining of DNA fragments.

The concentration of DNA in PCR, miniprep, digest, and ligation mixtures were quantified using a NanoDrop 3000 fluorospectrometer (Fisher Scientific) equipped with a nucleic acid analysis module. This step was crucial for ensuring the optimal DNA concentration at each step of the cloning process.

For transformation, *E. coli* HPS1 and DH5α, rendered competent by treatment with $CaCl_2$, were utilized. Transformation was achieved by introducing 5 µL of ligation mixture into the competent cells, followed by two minutes of heat shock at 42 °C and a subsequent two-minute cold shock at 4 °C to facilitate plasmid uptake. The transformed cells were then allowed to recover for one hour in nutrient-rich LB broth, incubated at 37 °C without agitation. For selection, the cells were plated on LB-agar containing 40 µg/mL X-gal, 0.1mM IPTG, and relevant antibiotics. Once plated, the transformations were incubated overnight at 37 °C and successful transformants were identified by either blue/white screening and/or antibiotic resistance, indicative of the presence of circular plasmids.

Putative transformants were further propagated in LB broth at 37 °C overnight. Plasmids from these cultures were extracted and purified using the Wizard® *Plus* SV Miniprep DNA Purification kit (Promega). Verified transformants were then preserved for long-term storage by suspending cultures, adjusted to an optical density of 0.2-0.6 OD_{600}/mL, in a 7:3 mixture of LB broth and glycerol solution and subsequently storing them at -80 °C.

Construction of pDR425 ΔPA5189 suicide vector

The deletion of the PA5189 gene in *Pseudomonas aeruginosa* was accomplished through a strategy of allelic exchange using a specifically designed recombinant suicide vector. This plasmid, pDR425, contained a truncated version of the PA5189 gene, and its construction was a three-step process. Initially, two precursor plasmids—pDR423 and pDR424—were constructed, encompassing flanking regions upstream and downstream of the PA5189 coding region, respectively. The subsequent combination of these regions in the ΔPA5189 suicide vector pDR425 resulted in a mutated version of PA5189, with the majority of its coding region effectively deleted. Thus, the construction of pDR425 thereby facilitated the eventual knockout of the PA5189 gene in *P. aeruginosa*.

The construction of pDR423 began with the PCR amplification of a DNA fragment from the region upstream of PA5189. This amplification used approximately 200 ng of wild-type PA01 genomic DNA as a template and 25mM of oDR261-262 forward and reverse primers (detailed in Table 1). The primers were annealed at 63 °C, in accordance with the recommendations provided by the NEB T_m calculator (tmcalculator.neb.com). This process resulted in the amplification of a 1,062 bp fragment containing the first ten residues of PA5189 and 1032 bp upstream, including the neighboring PA5188 gene as well as the noncoding region between the two genes. The oDR261-262 primer pair was designed to ensure that the amplified upstream region was flanked by *SacI* and *XbaI* restriction sites.

In parallel, the template recombinant suicide vector pEX18Tc (referenced in Table 1) was propagated in *E. coli* cultured in liquid LB media supplemented with 3 μg/mL tetracycline and incubated overnight at 37 °C with agitation. Post-propagation, pEX18Tc was extracted and purified via miniprep. Both the oDR261-262 amplicon and the pEX18Tc plasmid were digested with *XbaI* and *SacI*. Following purification of these digests, approximately 45 fmol of the oDR261-262 PA5189 upstream PCR product and 15 fmol of

the pEX18Tc plasmid were ligated. This ligation mixture was then transformed into *E. coli*

HPS1 λ pir (as listed in Table 1) using 5 µL of the ligation DNA. The putative transformants

were plated on LB-agar supplemented with 10 µg/mL tetracycline. Colonies resistant to

tetracycline and containing pDR423 were grown overnight at 37 °C in liquid LB broth

supplemented with 3 µg/mL tetracycline. Subsequently, pDR423 was purified via column

miniprep and digested with *NcoI* to verify the correct insertion of the amplicon into

pEX18Tc. The expected outcome was a 7,395bp plasmid, which upon restriction digestion

with *NcoI*, would yield fagments of 630 bp and a 6,765 bp.

Concurrently, pDR424, a cloning vector based on pUCP20-based and containing an

AmpR cassette, was constructed to harbor the downstream flanking region of PA5189. This

vector was constructed by cloning a 1,076 bp region downstream of PA5189 into pUCP20.

PCR amplification of approximately 200 ng of wild-type PA01 genomic DNA with oDR263

and oDR264 primers (Table 1) was conducted at an annealing temperature of 62 °C, as

recommended by the NEB T_m calculator for this primer pair. The amplified product included

the last nine residues of PA5189, the entirety of PA5190, and the first fifty residues of

PA5191, thus resulting in an insert comprising a PA5189 downstream flanking region.

Furthermore, the insert was flanked by *XbaI* and *HindIII* restriction sites. pUCP20 was

similarly propagated in *E. coli* cultured in LB broth and incubated overnight at 37 °C under

aerobic conditions. Post-propagation, pUCP20 was extracted and purified using the Wizard®

Plus SV Miniprep DNA Purification kit (Promega). Following this, both the pUCP20 vector

and the PA5189 downstream amplicon were digested by *XbaI* and *HindIII* using 0.25 U/µL

FD *XbaI* or FD *HindIII* (ThermoScientific™). Digested DNA was subjected to agarose gel

electrophoresis analysis to examine digestion efficacy. Subsequently, the *HindIII/XbaI*-

digested fragments were purified, ligated, and transformed into *E. coli* HPS1 λ pir (Table 1)

using 5 µL of ligation DNA. Putative transformants were selected on LB-agar plates

containing 100 µg/mL ampicillin for selection of colonies containing circularized pUCP20. Ampicillin-resistant colonies were then propagated overnight at 37 °C with shaking. Plasmids were extracted via miniprep and digested with *HindIII* and *SacI* to verify insertion of the 1,076 bp PA5189 downstream region amplicon.

In the subsequent phase of pDR425 ΔPA5189 recombinant suicide vector construction, precursor plasmids pDR423 and pDR424 underwent enzymatic digestion. The digestion of pDR423 with *XbaI* and *HindIII* enzymes yielded an expected 7,371 bp fragment, encompassing the pEX18Tc backbone and the upstream region flanking PA5189. Concurrently, pDR424 was digested to release an expected 1,083 bp fragment containing exclusively the oDR263-264-amplified PA5189 downstream flanking region. These digestion steps were crucial for preparing the fragments for their intended ligation.

Following the enzymatic digestions of pDR423 and pDR424, the resultant DNA fragments were subjected to agarose gel electrophoresis analysis for size verification, identification, and isolation of the desired DNA fragments. The specific fragments were excised and purified from the gel using a silica bead extraction method [46], thus removing any contaminants that could potentially interfere with the ligation process.

Following purification, the *HindIII/XbaI*-digested oDR263-264 PA5189 downstream fragment was ligated into similarly digested pDR423 plasmid. This ligation resulted in the strategic incorporation of the PA5189 downstream region into pDR423, a pEX18Tc vector already containing the PA5189 upstream region (refer to Table 1 and Figure 1 for detailed schematics). This precise assembly led to the formation of the pDR425 ΔPA5189 recombinant suicide vector.

The newly constructed pDR425 ligations were then introduced into *E. coli* DH5α λ pir (Table 1) via transformation. Putative transformants were plated on LB-agar supplemented with 10 µg/mL tetracycline for selection of colonies containing the circularized

plasmids, evidenced by their tetracycline resistance endowed by the pDR425 plasmid (*TcR*).

Colonies demonstrating tetracycline resistance were selected and cultivated overnight at 37

°C in LB-broth supplemented with 3 µg/mL tetracycline. Following this, pDR425 was

extracted from the cultured cells and purified. To confirm the successful insertion of the

1,076 bp oDR263-24 PA5189 downstream flanking region into pDR423, the purified

pDR425 was subjected to a final confirmatory digestion with *XbaI* and *HindIII*.

Construction of PA5189 Knockout Strain

The introduction of mutated PA5189 alleles into the *P. aeruginosa* genome was

executed through a triparental conjugation technique. This process involved the use of *E. coli*

DH5α and S17 as donor cells harboring the necessary plasmids, and the *P. aeruginosa* PA01

strain as the recipient. While plasmids such as pDR425 and pDR428, along with pHERD26T,

are not inherently capable of transferring into PA01 independently, their transfer was

facilitated using a helper strain of *E. coli*, pRK2013 (as delineated in Table 1).

The preparatory phase for triparental conjugation involved culturing the *E. coli* strains

in LB broth supplemented with specific antibiotics: 3 µg/mL tetracycline for *E. coli*

DH5α(pDR425) and *E. coli* S17(pHERD26T), 10 µg/mL gentamicin for *E. coli*

DH5α(pDR426) and *E. coli* DH5α(pDR428), and 50 µg/mL kanamycin for *E.*

coli(pRK2013). All *E. coli* strains were incubated overnight at 37 °C under aerobic

conditions. Concurrently, *P. aeruginosa* strains were propagated in LB broth overnight at 42

°C with shaking, following the protocol established by Rolfe et al. [16].

For the conjugation experiments, donor, helper, and recipient strains were combined

in a 10:2:1 ratio within a 1 mL sterile saline solution. The conjugation process was carried out

as per the method described in 2001 by Green and Sambrook [15]. Post-conjugation, the

resultant transconjugant cultures were resuspended and spread on selective PIA-agar plates.

These plates were supplemented with 100-150 µg/mL tetracycline, contingent upon the specific plasmid and strain conjugations. Incubation of these plates was conducted for 12-36 hours at 37°C to facilitate colony growth.

Following this incubation, colonies that exhibited resistance to tetracycline (*TcR*) were selected, as tetracycline resistance conferred by the vector facilitates the selection of merodiploid intermediates, where both the wild-type and disrupted alleles of PA5189 coexist [9, 28]. These merodiploid colonies were then restruck on LB-agar supplemented with 10% sucrose, thus providing a counter-selection against the maintenance of the vector sequence as the *sacB* gene in the vector (see Figure 1) encodes an enzyme lethal to *P. aeruginosa* in the presence of sucrose. This step was aimed at promoting double-crossover events leading to the resolution of the merodiploid state, a crucial aspect of successful allelic exchange [9]. This sucrose-triggered recombination ensured that only bacteria which have lost the pDR425 vector, either reverting to wild-type or with PA5189 knocked out, can survive.

The successful knockout of PA5189 in PA01 was initially assessed phenotypically. Double-crossover recombinants exhibiting loss of *TcR* (and/or *GmR* in PA01-428 conjugants). To confirm the genotypic alteration, PCR analysis was conducted using primers oDR265 and oDR266. This analysis was designed to generate distinct amplicons of D 3,179, 3,400, and 2,886 bp from wild-type PA01, PA01-428 (PA01-PA5189 UP::*GmR),* and PA01-425 (ΔPA5189) genomic DNA templates, respectively. The size differentiation of these amplicons served as a definitive marker for verifying the genetic modification in the native *P. aeruginosa* genome.
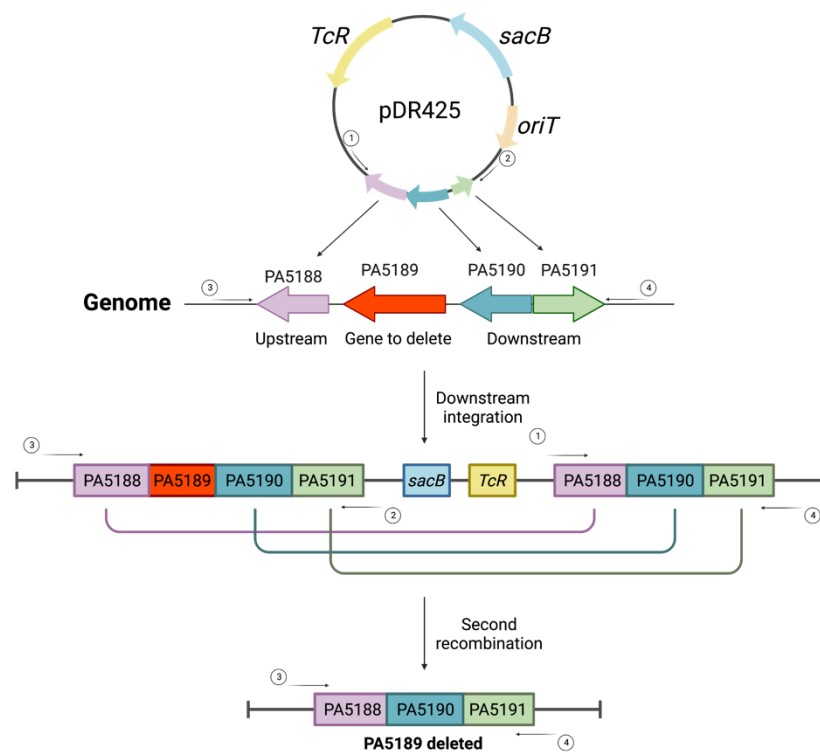
Figure 1. Double recombination events yield PA01(pDR425) P. aeruginosa conjugants experiencing knockout of PA5189. Inspired by Figure 4 from Huang and Wilks, (2017) [28]. pDR425 utilizes pEX18Tc double allelic exchange machinery resulting in downstream integration of the plasmid in the host genome and formation of merodiploid transconjugants. Secondary recombination events are triggered by plating *TcR* merodiploid colonies on LB+10% sucrose, yielding knockout of PA5189. ① denotes hybridization with oDR265, ② denotes hybridization with oDR266, ③ denotes hybridization with oDR261, and ④ denotes hybridization with oDR264 (Table 1). pDR426 uses similar construction and integration to pDR425 for knockout of PA5189, except for introduction of a 534bp *aacC1 GmR* cassette between PA5188 and PA5190. pDR428 [29] also utilizes pEX18Tc-based construction, although they utilize upstream integration to insert an *aacC1 GmR* mariner transposon upstream of PA5189, which is not disrupted or knocked out after dual recombination events.

Minimum inhibitory assay

For the MIC assay, ingle colonies of *P. aeruginosa* strains were inoculated into cation-adjusted Mueller-Hinton (CAMH) broth and incubated overnight at 37 °C with constant agitation. The overnight cultures were then subcultured in fresh CAMH broth to achieve logarithmic-phase growth, indicated by an optical density at 600 nm (OD_{600}) of 0.1-0.6 OD_{600}/mL. The OD_{600} of the subcultures was adjusted via dilution in fresh CAMH broth to

approximately 0.01 using a calibrated spectrophotometer to ensure inocula of approximately 1×10^6 CFUs/mL. Antibiotics selected for the study were solubilized following the manufacturer's guidelines and subjected to twofold serial dilutions in sterile water (pH 7) to establish a concentration gradient.

In a sterile, flat-bottom 96-well microtiter plate (Fisher), each well received a combination of antibiotic solution and bacterial cell suspension at a ratio of 1:10. A positive control (bacteria treated with a volumetric equivalent of sterile water) was included to assess potential contamination. The plates were then sealed with plate sealer to prevent evaporation and contamination and incubated at 37 °C overnight. Post-incubation, the OD_{600} was measured using a microplate reader (BioTek). The MIC was determined as the lowest antibiotic concentration at which bacterial growth was inhibited in comparison to the growth control. This assay was conducted in triplicate for each antibiotic and strain combination to promote reproducibility and accuracy.

Kirby-Bauer disc diffusion assay

In this assay, single colonies of *P. aeruginosa* strains were initially grown in Mueller-Hinton (MH) broth and incubated overnight at 37 °C with agitation. The overnight cultures were then subcultured in fresh MH broth until logarithmic-phase growth was achieved (OD_{600}/mL 0.1-0.6). The OD_{600} of the subcultures was then adjusted to approximately 0.01 using a spectrophotometer to ensure standardized inocula of approximately 1×10^6 CFUs/mL. MH agar plates were uniformly inoculated with the standardized bacterial suspension using sterile 3/16" cotton-tipped applicators (ULINE). Antibiotic discs were placed onto the inoculated MH-agar plates using sterile forceps, ensuring proper spacing to prevent overlapping of inhibition zones. The plates were incubated overnight at 37 °C.

Post-incubation, the diameter of the zones of inhibition surrounding each disc was measured in millimeters using a calibrated ruler. Each zone was measured five time to calculate an average value, mitigating measurement variability. The experiment was replicated three times for each strain and antibiotic combination.

Table 1. Strains, plasmids, and oligonucleotide primers used in this study.

Name	Relevant characteristics/plasmid construction	Reference/Source
Strains		
E. coli DH5α	Cloning strain	Unknown Liss, 1987
E. coli S17	Cloning strain	Unknown Simon et al 1986
E. coli HPS1	Cloning strain	Unknown
E. coli pRK2013	Triparental conjugation helper strain	Unknown
E. coli pHERD26T	*E. coli* with pUCP20-based conjugable vector	Unknown
PA01	Sequenced wild-type laboratory strain	[10]
PA01-425	ΔPA5189	This study
PA01-428	PA01-PA5189 UP::*GmR*	This study
F2	PA01-PA5189 UP::*GmR pmrB*^{M186T}	This study
Plasmids		
pUCP20	*AmpR* cloning vector	Unknown
pEX18Tc	*TcR, oriT, sacB*, gene replacement suicide vector with MCS from pUC18	[9]
pDR423		
pDR424	pUCP20 with 1076bp PA5189 downstream region from PA01 flanked by *HindIII* and *XbaI* sites	
pDR425	pEX18Tc containing in-frame deletion from residues 1-302	This study
pDR428	pEX18Tc containing PA5189 UP::*GmR* from F2	This study
Primers		
oDR263	(5'- CAGTCTAGAGCTGGTCGAACAGATCC-3') upstream primer; creates *XbaI* site for PA5189 knockout	This study
oDR264	(5'- GCTAACGTTCCCTTGCTTTCGTCTTG-3'); downstream primer; creates *HindIII* site for PA5189 knockout	This study
oDR265	(5'-TCGATGTCGGCACTACG-3') PA5189 upstream check primer	This study
oDR266	(5'- CATCGAACGGATGCTGAC-3') PA5189 downstream check primer	This study

Biofilm formation assay

In the biofilm formation assay, single colonies of *P. aeruginosa* strains were cultivated in CAMH broth and incubated overnight at 37 °C with agitation. The overnight cultures were subcultured in fresh CAMH broth until reaching logarithmic-phase growth (OD_{600}/mL of 0.1-0.6). The OD_{600} of the subcultures was then adjusted to approximately 0.01 OD_{600}/mL in LB, TS, and CAMH broth using a spectrophotometer, thus standardizing the inocula to approximately 1×10^6 CFUs/mL. The microtiter plate method was employed to assess biofilm production [47]..Standardized bacterial suspensions were dispensed into sterile flat-bottom 96-well microtiter plates (Fisher) and sealed to prevent evaporation and contamination. The cultures were incubated aerobically at 37 °C in a stationary position overnight.

Following incubation, planktonic cells were removed from the plate, and each well was rinsed three times with non-sterile water to eliminate non-adherent bacteria and extracellular matrix. Each well was then stained with 125 µL of 0.1% crystal violet (Difco) for ten minutes at room temperature. Post-staining, the plates were thoroughly rinsed and allowed to dry. The crystal violet bound to the biofilms was solubilized in 200 µL of 30% glacial acetic acid and transferred to a new microtiter plate. The biofilm formation index was quantitatively assessed by measuring the absorbance at 550 nm using a microplate reader (BioTek).

Results

Construction of the pDR425 ΔPA5189 suicide vector

This study endeavored to elucidate the role of the PA5189 gene in *Pseudomonas aeruginosa* by analyzing mutants experiencing altered expression of PA5189. The creation of site-specific ΔPA5189 mutants in *P. aeruginosa* necessitated the development of a two-step

allelic exchange protocol. Central to this process was the design of the pEX18Tc-based suicide vector, pDR425, which was engineered to facilitate the knockout of PA5189 in the wild-type PA01 strain of *P. aeruginosa* (refer to Figure 1). The construction of pDR425 required the strategic cloning of flanking regions both upstream and downstream of the PA5189 locus from PA01 genomic DNA. This cloning was a crucial step in preparing for eventual allelic exchange via dual homologous recombination (illustrated in Figure 1).

In the preliminary phase, the upstream flanking region of PA5189 was cloned into pEX18Tc to create the pDR423 plasmid. Simultaneously, the downstream flanking region of PA5189 was cloned into the ampicillin-resistant expression vector pUCP20 (Figure 2). Subsequent steps involved the excision of the downstream region from pDR424 and its ligation into pDR423. This manipulation of precursor plasmids culminated in the formation of pDR425, a suicide vector harboring both the upstream and downstream flanking regions of PA5189, primed for the seamless deletion of this gene via allelic exchange.

The construction of pDR425 necessitated commenced with the assembly of its predecessor pDR423. A specific fragment located upstream of the PA5189 gene in the wild-type PA01 genomic DNA of *P. aeruginosa* was cloned into the pEX18Tc vector (details in Table 1) [28]. The pEX18Tc vector was extracted and purified using a column miniprep, and agarose gel electrophoresis analysis revealed a distinct band, corresponding approximately to its expected size of 6,349 bp (Figure 2A).

In parallel, the PCR amplification of a 1,062 bp flanking region upstream of PA5189 was subjected to gel electrophoresis analysis, revealing a band aligning closely with the anticipated size (Figure 2B). Both the purified pEX18Tc plasmid DNA and the amplified PA5189 upstream region were then digested with *SacI* and *XbaI* restriction enzymes. Gel electrophoresis of these digested products indicated the presence of major fragments, matching the expected lengths of 3,874 bp for the digested pEX18Tc and 1,059 bp for the

PA5189 upstream flanking region (Figure 2C). The digested fragments, post-electrophoresis, were purified using silica bead extraction and were subsequently ligated and transformed into *E. coli* DH5α λ pir (Table 1).

The resultant pDR423 construct was extracted from tetracycline-resistant *E. coli* colonies and purified via column miniprep. A subsequent restriction digest was performed using *EcoRI* to verify the correct insertion of the upstream fragment into pDR423. The products of this digestion were analyzed through gel electrophoresis, which displayed bands closely corresponding to the expected sizes of 1,059 bp and 6,365 bp, indicative of successful cloning (Figure 2D).

In conjunction with the construction of pDR423, the creation of pDR425 necessitated the cloning of a flanking region downstream of the PA5189 gene from the wild-type PA01 genomic DNA of *P. aeruginosa* into pEX18Tc. To initiate this phase, pDR424 was first constructed by cloning a DNA fragment that included a downstream flanking region of PA5189 into a high-copy number ampicillin resistant expression vector pUCP20 (see details in Table 1). Upon purification of pUCP20 using a column miniprep technique, gel electrophoresis analysis confirmed the presence of a band corresponding to the expected size of the plasmid, approximately 3,898 bp (Figure 2A).

Simultaneously, PCR amplification of a 1,076 bp fragment, encompassing the downstream flanking region of PA5189, was analyzed. Gel electrophoresis analysis of this PCR product revealed a distinct band aligning with the projected size (Figure 2B). Following purification, both the pUCP20 plasmid DNA and the PA5189 downstream amplicon were subjected to restriction digestion with *HindIII* and *XbaI* enzymes. Gel electrophoresis of these digested samples yielded bands that approximated the expected sizes of the major fragments – 3,874 bp for the plasmid and 1,076 bp for the amplicon (Figure 2C). Subsequent ligation of these *HindIII*/*XbaI*-digested fragments, followed by transformation into *E. coli* DH5α λ pir,

resulted in the completed assembly of pDR424. The pDR424 construct was extracted and

purified, with the insertion of the downstream fragment confirmed through *HindIII* and *SacI*

restriction digestion. The resulting gel electrophoresis analysis displayed bands consistent

with the anticipated fragment sizes of 1,108 bp and 3,849 bp (Figure 2E).
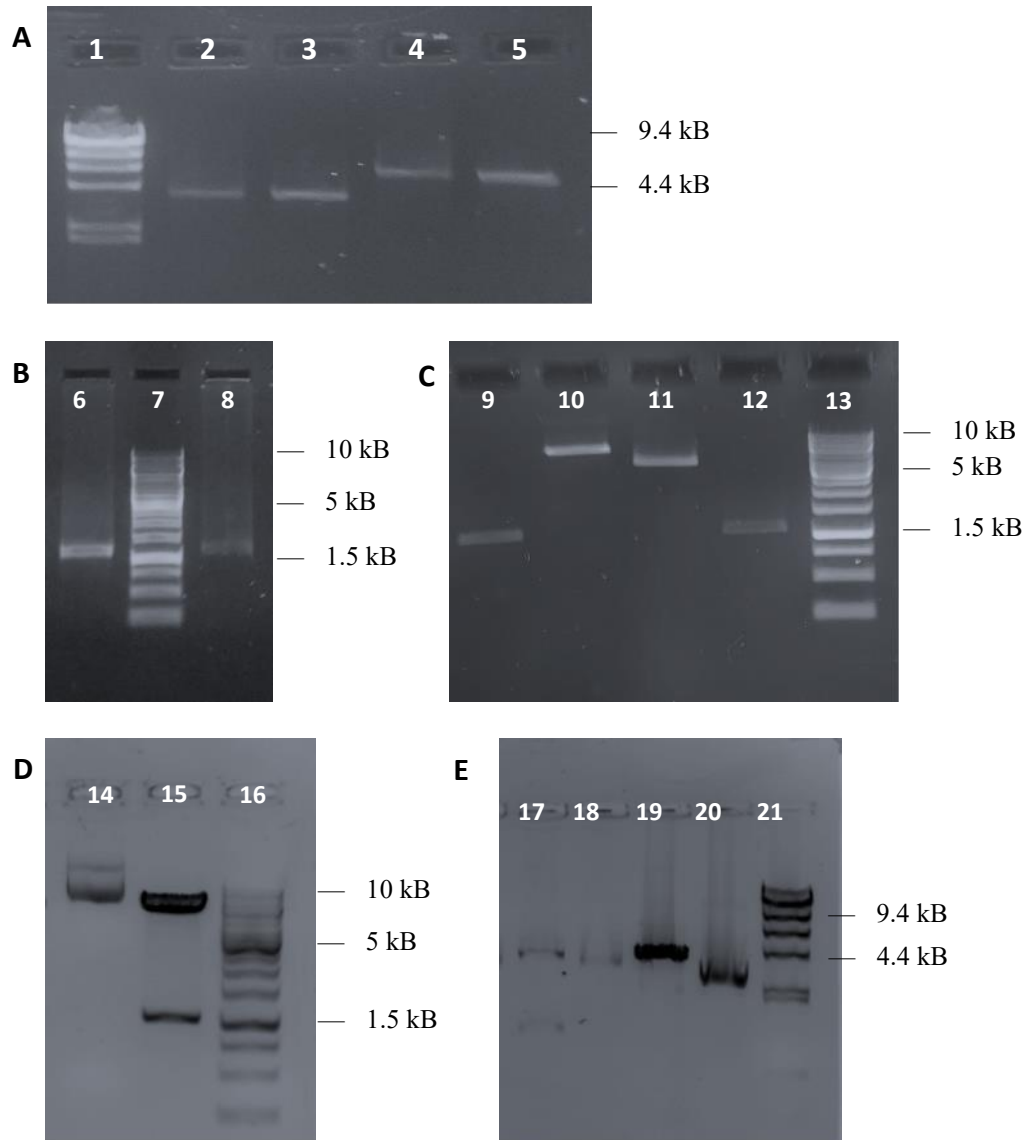
***Figure 2. Construction of pDR423-424*. A)** *Purification of parent plasmids pUCP20 and pEX18Tc.* 1: 2.5μg Lambda DNA/*HindIII* marker (ThermoFisher), 2: purified pUCP20 (3,898bp), 3: Column miniprep-purified pUCP20 (3,898bp), 4: impurified pEX18Tc (6,349bp), 5: column miniprep-purified pEX18Tc (6,349bp). **B)** *PCR amplification of upstream and downstream regions of PA5189 using 200ng PA01 genomic DNA template.* 6: 1,062bp band amplified from upstream region of PA5189 using oDR261-262. 7: 5μg GeneRuler 1kB ladder (Fisher). 8: 1,076bp band amplified from downstream region of PA5189 using oDR263-264. **C)** *Restriction digestion of plasmids and insert fragments.* 9: *XbaI/SacI*-digested 1,059bp PA5189 upstream fragment. 10: *XbaI/SacI*-digested pEX18Tc (expected 6,234bp and 25bp fragments). 11: *HindIII/XbaI*-digested pUCP20 (expected 24bp and 3,874bp fragments). 12: *HindIII/XbaI*-digested 1,076bp PA5189 downstream fragment.

13: 5µg GeneRuler 1kB ladder (ThermoFisher). **D)** *Verification of pDR423 using EcoRI restriction digestion.* 14: *EcoRI*-digested pEX18Tc. Expected a 630bp and a 6,765bp fragment. 15: *EcoRI*-digested pDR423. pDR423 was extracted and purified via column miniprep after ligation of pEX18Tc with the 1,059bp PA5189 upstream fragment and transformation into *E. coli* DH5α competent cells. Digestion with *EcoRI* yields expected fragment sizes of 1,030bp and 6,365bp. 16: 5µg GeneRuler 1kB ladder (Fisher).**E)** *Verification of pDR424 using HindIII/SacI restriction digestion.* 17: *HindIII/SacI*-digested pDR424. pDR424 was extracted and purified via column miniprep after ligation of pUCP20 with the 1,076bp PA5189 downstream fragment and transformation into *E. coli* DH5α competent cells. Digestion with *HindIII* and *SacI* yields expected fragment sizes of 1,108bp and 3,849bp. 18: Undigested pDR424 (4,957bp). 19: *HindIII/SacI*-digested pUCP20. Expected a 49bp and a 3,849bp fragment. 20: Undigested pUCP20 (3,898bp). 21: 2.5µg Lambda DNA/*HindIII* marker (ThermoFisher).

With pDR423 and pDR424 successfully constructed and verified, the next pivotal involved the excision of the PA5189 downstream region from pDR424 and its subsequent cloning into pDR423. This process culminated in the creation of pDR425, a pEX18Tc-based suicide vector containing both upstream and downstream flanking regions of PA5189, poised to facilitate allelic recombination in the *P. aeruginosa* wild-type PA01 genome (illustrated in Figure 1). Gel electrophoresis analysis of *HindIII/XbaI-digested* pDR423 yielded fragments closely matching the expected sizes of 7,371 bp and 24 bp, the latter of which was not visible due to its size (Figure 3A). Similarly, the *HindIII/XbaI* digestion of pDR424 also generated fragments congruent with the predicted sizes of 1,083 bp and 3,874 bp (Figure 3B).

These *HindIII/XbaI*-digested fragments, derived from both pDR423 and PDR424, underwent silica bead purification to remove non-nucleic acid contamination and other impurities. Analysis of the purified *HindIII/XbaI*-digested pDR423 containing the PA5189 upstream region exhibited a singular band indicative of a size of approximately 8,433 bp (Figure 3C). Moreover, the purified DNA fragment encompassing the PA5189 downstream region displayed a band corresponding to an expected size of around 1,083 bp (Figure 3D). pDR425 was then extracted and purified via column miniprep following the ligation of these digested fragments and their subsequent transformation into *E. coli* DH5α λ pir. The candidates for pDR425 transformants were scrutinized for insertion of the PA5189

downstream fragment derived from pDR424. Verification was performed through *XbaI*

restriction digestion, and gel electrophoresis analysis of the digested pDR425 revealed a

single band, indicating the anticipated length of the pDR425 construct, approximately 8,454
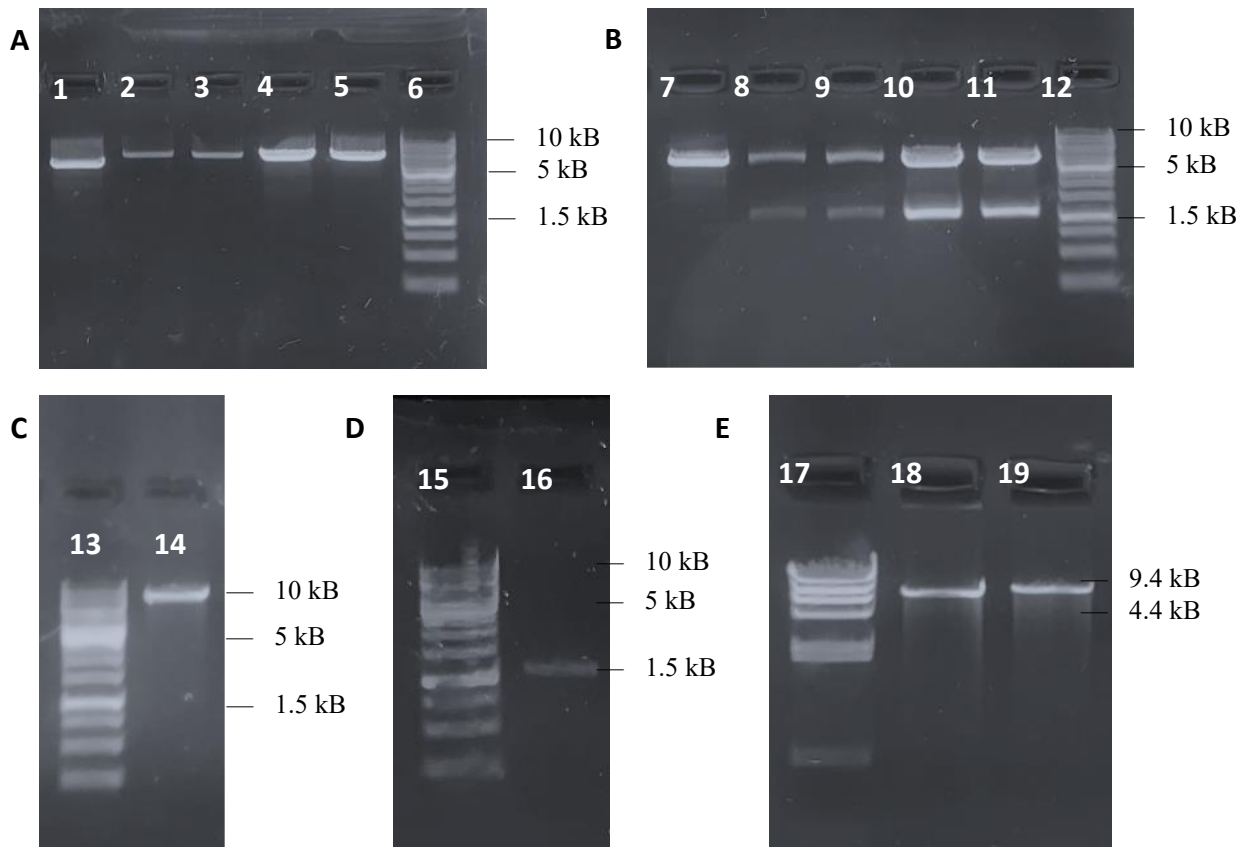
bp (Figure 3D).

Figure 3. Construction of pDR425. **A)** *Restriction digestion of pDR423 with HindIII and XbaI*. 1: Undigested pDR423 (7,395bp). 2-5: *HindIII/XbaI*-digested pDR423. Expected fragment sizes of 24bp and 7,371bp. 6: 5µg GeneRuler 1kB ladder (ThermoFisher). **B)** *Restriction digestion of pDR424 with HindIII and XbaI*. 7: Undigested pDR424 (4,957bp). 8-11: *HindIII/XbaI*-digested pDR424. Digestion yields expected fragment sizes of 1,083bp and 3,874bp. 12: 5µg GeneRuler 1kB ladder (ThermoFisher). **C)** *Purification of HindIII/XbaI-digested pDR423 for construction of pDR425*. 13: 5µg GeneRuler 1kB ladder (ThermoFisher). 14: Silica bead purified *HindIII/XbaI* digested pDR423 (7,371bp fragment containing pEX18Tc DNA with insertion of 1,062bp PA5189 upstream region). Expected one fragment that is 8,433bp in length. **D)** *Purification of HindIII/XbaI-digested PA5189 downstream region from pDR423 for insertion into pDR423*. 15: GeneRuler 1kB ladder (ThermoFisher). 16: Silica bead purified *HindIII/XbaI* digested pDR424 (1,083bp PA5189 downstream region fragment excised from pUCP20). **D)** *Restriction digest of pDR425 with XbaI*. **E)** *Restriction digestion of pDR425 with XbaI*. 17: 2.5µg Lambda DNA/*HindIII* marker (ThermoFisher). 18-19: *XbaI*-digested pDR425. The downstream region excised from pDR424 was ligated into pDR423 and transformed into *E. coli* HPS1 λ pir (see **Table 1**) to create pDR425. pDR425 was then purified via column miniprep and digested with *XbaI*.

Genotypic verification of knockout of PA5189 in PA01

Post-transformation into *E. coli*, the pDR425 construct underwent a series of verifications to ensure its structural integrity and functional capacity. This process was pivotal, as pDR425 was engineered to facilitate a seamless allelic exchange in *P. aeruginosa* through tetracycline resistance and sucrose-triggered double recombination events, utilizing elements embedded within the pEX18Tc suicide vector.

Following the verification of pDR425 in *E. coli* (see Figure 3), the vector was prepared for triparental conjugation into *P. aeruginosa*. Allelic exchange events in the PA01 genome were then facilitated first by *TcR* selection of *P. aeruginosa* PA01 colonies containing pDR425, thus ensuring successful conjugation and selection of merodiploid intermediates. Subsequently, exposure to sucrose ensured counterselection against the maintenance of the pDR425 vector, thus leading to the resolution of the merodiploid state and seamless allelic exchange facilitated by pDR425.

The successful incorporation of pDR425 into the PA01 strain, leading to the targeted knockout of the PA5189 gene, was a critical juncture in this study. To verify this knockout genotypically, PCR analysis was conducted using the primer pair oDR265-266 (referenced in Table 1). This primer pair was strategically designed for specificity: oDR265 anneals to a sequence upstream of the PA5189 locus, while oDR266 binds to a downstream region. Consequently, the length of the resulting PCR amplicon serves as an indicator of the successful deletion of PA5189 in the putative PA01-425 conjugants.

Gel electrophoresis was utilized to analyze the PCR-amplified genomic DNA from PA01-425 conjugants. A distinct band was observed in the gel, which corresponded approximately to the expected amplicon length of 2,886 bp (Figure 4). This observation strongly suggested that the PA5189 gene had been successfully excised from the genome of PA01.

Additionally, for comparative purposes, genomic DNA from both the wild-type PA01 and the PA01-428 strain, which harbors the PA5189 UP::*GmR* modification, were also subjected to PCR under identical conditions. The resulting amplicons from these strains appeared to be commensurate with, or slightly larger than, the anticipated lengths of 3,179 bp for the PA01 wild-type and 3,400 bp for the PA01-428 strain, respectively. It is important to note, however, that the interpretation of these results was somewhat complicated by anomalies in the gel electrophoresis. Specifically, issues such as warping of the gel and suboptimal quality of the DNA ladder employed for size estimation introduced challenges in precisely determining the amplicon sizes. These factors somewhat obscured the clarity of the results and necessitated cautious interpretation of the data.

In summary, the PCR and gel electrophoresis analyses provided strong genotypic evidence for the successful knockout of PA5189 in the PA01-425 strain of *P. aeruginosa*. While minor electrophoretic anomalies presented interpretative challenges, the overall pattern of the bands observed was consistent with the hypothesized genomic alterations.

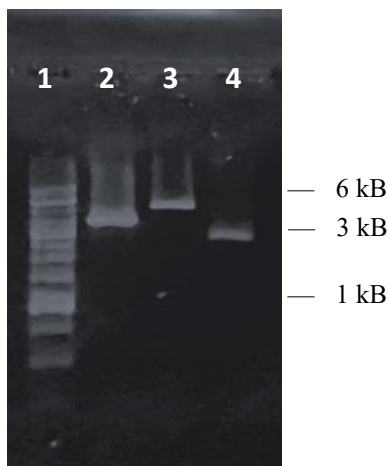***Figure 4. Genotypic verification of ΔPA5189 mutants.*** 1: 5μg GeneRuler 1kB ladder (ThermoFisher), 2: PCR amplification of PA01 genomic DNA using primer pair oDR265-266. Expected a 3,179bp fragment. 3: PCR amplification of PA01-428 genomic DNA using primer pair oDR265-266. Expected a 3,400bp fragment. 4: PCR amplification of PA01-425 genomic DNA using primer pair oDR265-266. Expected a 2,886bp fragment.

Assessment of antibiotic susceptibility of PA5189 perturbation strains

In order to elucidate the impact of PA5189 expression perturbations on antibiotic susceptibility in *P. aeruginosa*, comprehensive Kirby-Bauer disc diffusion assays and microbroth minimum inhibitory concentration (MIC) tests were conducted. These assays were performed using a range of commonly used broad-spectrum antibiotics, providing insights into the implications of both knockout and overexpression of the PA5189 gene in *P. aeruginosa*.

The Kirby-Bauer disc diffusion assays revealed that for the PA01-425 strain which contains the ΔPA5189 knockout, there was a negligible deviation in the zones of inhibition compared to the wild-type PA01 strain across all six antibiotics tested (Table 2). This similarity in antibiotic sensitivity between the knockout strain and the wild-type indicates that the deletion of PA5189 might not significantly alter the bacterium's inherent antibiotic resistance profile for these antibiotics.

In stark contrast, the PA01-428 strain, characterized by the overexpression of PA5189, exhibited a pronounced reduction in the zones of inhibition, particularly when exposed to ciprofloxacin and imipenem (Table 2). This decrease in the zone of inhibition suggests an increased resistance pattern in the PA01-428 strain towards these specific antibiotics, suggesting a potential role of PA5189 overexpression in conferring antibiotic resistance.

Complementing these observations, the results of the MIC assays conducted with colistin, tobramycin, and tetracycline revealed minimal differences among the strains. The MIC values for these antibiotics were consistently similar across the wild-type, ΔPA5189 knockout, and PA5189 overexpression strains (Table 2), indicating less than a twofold difference in MIC values across all antibiotics. This suggests that the perturbation of PA5189, either by knockout or overexpression, does not substantially affect the bacterial susceptibility to these antibiotics.

Furthermore, the data derived from both Kirby-Bauer disc diffusion and MIC assays collectively suggest differential expression of PA5189 does not markedly influence the sensitivity of *P. aeruginosa* to colistin, tetracycline, or ceftazidime (Table 2).

In summary, our findings indicate that the knockout of PA5189 does not significantly alter antibiotic susceptibility in *P. aeruginosa*, while its overexpression appears to confer increased resistance specifically to ciprofloxacin and imipenem. The consistency of these observations across different antibiotics and assay techniques underscores the likely role of PA5189 in the antibiotic resistance mechanisms of *P. aeruginosa*, warranting further investigation to elucidate its precise function in the context of antimicrobial susceptibility.

Table 2. Result of Kirby-Bauer disc diffusion and MIC assays.

Drug	Diameter of zone of inhibition (mm)[B]			MIC (µg/mL)[C]		
	PA01	PA01-428	PA01-425	PA01	PA01-428	PA01-425
Colistin	17.9	18.4	18.8	4	4	4
Tobramycin	22.3	21.1	24.7	0.25	0.75	0.5
Ciprofloxacin	26.7	17.6	27.6	---	---	---
Tetracycline	9.5	9.15	7.9	100	100	100
Ceftazidime	28.8	28.7	28.5	---	---	---
Imipenem	22.2	15.8	23.9	---	---	---

[A]The following discs were used in Kirby-Bauer disc diffusion: CT10, NN10, CIP5, TE30, CZ30, and IPM10.
[B]The diameter of zone of inhibition (mm) was measured as an average of 5 measurements per 3 technical replicates of 2 biological replicates.
[C]MIC was analyzed as an average of three technical replicates.

Assessment of biofilm-forming capacities of PA5189 perturbation strains

This segment of the study inquired as to whether modification of the PA5189 gene, either through loss or overexpression, significantly affects the biofilm-forming capabilities of *P. aeruginosa*. We employed a quantitative assay measuring the production of polysaccharides, a key component of biofilms, by three *P. aeruginosa* strains: the wild-type PA01, PA01-425 (ΔPA5189 knockout), and PA01-428 (PA5189 overexpression).

We observed negligible differences in biofilm formation among the three strains when cultivated in LB Miller broth (Figure 5). The spectrophotometric absorbance readings at 630

nm (A_{630}), obtained post-staining with Crystal Violet, were notably similar across all strains. This uniformity suggests that in LB medium, biofilm formation is relatively low and consistent, irrespective of the PA5189 gene expression status.

In contrast, a divergent biofilm formation pattern was noted when cultivated in Tryptic Soy (TS) broth and cation-adjusted Mueller-Hinton (CAMH) broth media. Specifically, the PA01-428 strain, characterized by overexpression of PA5189, demonstrated an elevated level of biofilm formation compared to the wild-type PA01 and the PA01-425 knockout strain when grown in TS broth (Figure 5). Conversely, in CAMH broth, PA01-428 exhibited significantly reduced biofilm formation compared to the wild-type PA01 and PA01-425 ΔPA5189 strains (Figure 5).

In parallel, biofilm formation in the PA01-425 ΔPA5189 knockout strain was closely matched with that of the wild-type PA01 across all three media types included in this study (Figure 5). This consistency suggests that the absence of PA5189 does not markedly influence the biofilm-forming capacity of *P. aeruginosa* under these growth conditions.
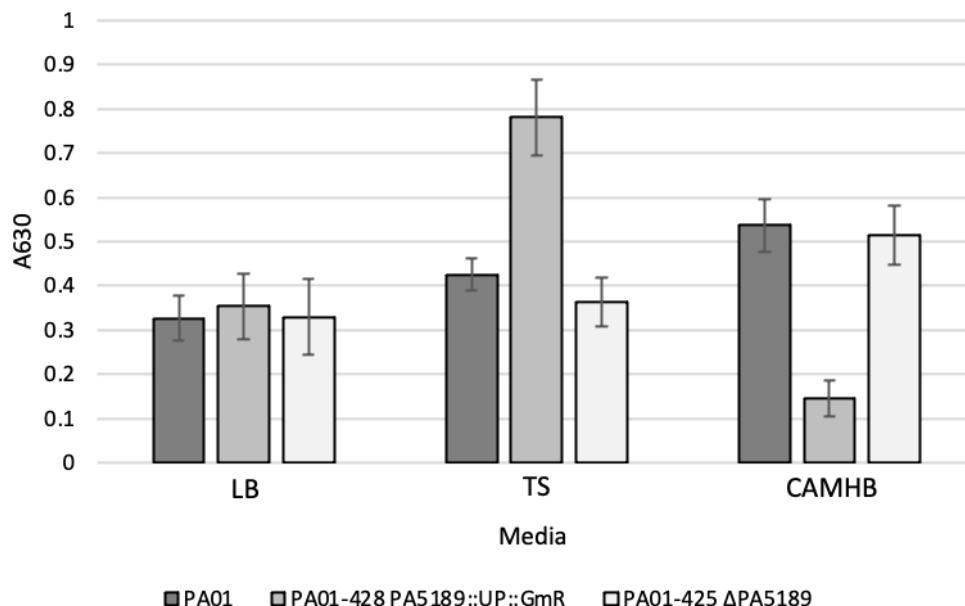

Figure 5. Biofilm formation assay of P. aeruginosa strains experiencing differential expression of PA5189. Biofilms of PA01 (dark grey), PA01-428 (medium grey), and PA01-425 (light grey) were cultivated in 96-well microplates for 24 hours at 37°C in LB, TS, and cation-adjusted MH broth (CAMHB). Biofilm formation was quantified via visible light

spectrophotometry at 630nm using a 96-well microplate Crystal violet staining technique (Methods). Each bar represents the geometric average of eight technical replicates. Error bars denote ±1 standard deviation from the geometric average.

Discussion

The rationale behind this investigation was fundamentally aimed at characterizing the role of the PA5189 gene in *Pseudomonas aeruginosa*, with a specific focus on its involvement in antibiotic resistance and biofilm formation. This was pursued through the construction of pDR425, a plasmid designed to knockout PA5189, as well as its predecessors pDR423 and pDR424. After introducing the PA5189 knockout allele into the *P. aeruginosa* genome, we sought to characterize the antibiotic resistance and biofilm formation profiles of strains experiencing differential expression of PA5189.

Creating and verifying the PA01-425 ΔPA5189 knockout strain

The construction of PA01-425 was achieved by harnessing traditional molecular cloning methods to insert upstream and downstream flanking regions of PA5189 into a pEX18Tc-based recombinant suicide vector and a cloning vector, which were combined to create the pDR425 vector. The successful creation of pDR425 and its precursor plasmids was evidenced by sizes of fragments obtained after PCR amplification and restriction digestion, followed by agarose gel electrophoresis. Following successful construction of pDR425, triparental conjugation was employed to introduce the plasmid and induce recombination of the knockout allele into the *P. aeruginosa* PA01 genome. The expected reduction in the size of the PCR-amplified PA5189 gene post-use of pDR425 provided preliminary evidence of successful knockout in the PA01-425 strain. Upon integrating pDR425 into *P. aeruginosa*, we embarked on a comparative study involving strains with wild-type PA5189 expression (PA01), PA5189 knockout (PA01-425), and PA5189 overexpression (PA01-428). The

differential expression of PA5189 in these strains was subsequently assessed through minimum inhibitory concentration, Kirby-Bauer disc diffusion, and biofilm formation assays.

During construction of the pDR423-425 plasmids, agarose gel electrophoresis of the pDR425 and pDR425-precursor pDR423 and pDR423 constructions was approximately correct but failed to provide comprehensively accurate analyses of the sizes of fragments generated after PCR and restriction digestion, although the general trends between the distance travelled of fragments of interest and the distance travelled by the bands in the GeneRuler 1kB ladder and the Lambda DNA/*HindIII* standard remained relatively consistent (Figures 2-3). In addition, discrepancies on the gel between undigested, digested, and purified plasmids can also be attributed to supercoiling of the plasmid DNA, causing undigested plasmids to appear smaller than linearized plasmids due to mitigation of friction caused by a decrease in the surface area interacting with the agarose matrix [45]. Moreover, verification of PA01-425 using the primer pair oDR265-266 (Table 1, Figure 4), later confirmed knockout of PA5189 in PA01 and, retroactively, proper construction of pDR425.

Characterizing the role of PA5189 in mediating drug sensitivity

In this study, the genetic manipulation of the PA5189 gene in wild-type PA01 *P. aeruginosa* provided a unique opportunity to elucidate its role in mediating drug sensitivity. This was explored through comprehensive minimum inhibitory concentration (MIC) and Kirby-Bauer disc diffusion assays across strains exhibiting differential expression of PA5189. Notably, the disc diffusion assays revealed intriguing trends: both PA01-425 (ΔPA5189) and PA01-428 (overexpression PA5189) displayed sensitivities to colistin, tobramycin, tetracycline, and ceftazidime that were comparable to the wild-type strain. This observation, documented in Table 2, implies a degree of functional redundancy or non-essentiality of PA5189 in the resistance mechanisms against these antibiotics.

Contrastingly, we observed a significant decrease in sensitivity to imipenem and ciprofloxacin in PA01-428, suggesting that overexpression of PA5189 may confer heightened resistance to these particular antibiotics. This phenomenon was not mirrored in the ΔPA5189 strain, as PA01-425 exhibited a drug sensitivity profile similar to that of the wild-type. The absence of noticeable changes in MIC values for colistin, tobramycin, and tetracycline (Table 2) further corroborates the specificity of PA5189's influence on imipenem and ciprofloxacin resistance. Imipenem and ciprofloxacin target key bacterial processes – cell wall biosynthesis and topoisomerase II activity, respectively – leading to cell lysis and inhibition of DNA replication [48, 49]. The lack of prior research directly linking PA5189 to these cellular functions suggests a previously unexplored aspect of *P. aeruginosa*'s antibiotic resistance mechanisms. Our findings propose that PA5189 may be part of a regulatory network that either mediates or significantly impacts these processes and potentially influencing the bacterial response to antibiotics. This might further extend to the modulation of drug entry or export mechanisms, a hypothesis that warrants further investigation.

 Furthermore, the negligible impact on drug resistance following deletion of PA5189 posits that this gene may not be highly expressed under standard conditions. This observation aligns with significant alterations in antibiotic sensitivity only being evident upon PA5189 overexpression. The differential expression of PA5189 and its selective impact on antibiotic resistance profiles, particularly to imipenem and ciprofloxacin, underscore its potential role in a complex regulatory network that mediates *P. aeruginosa*'s response to antibiotics.

Investigating the biofilm formation profile of PA5189 expression mutants

In concordance with our exploration of drug sensitivity, we extended our investigation to understand the influence of PA5189 expression on biofilm formation in *Pseudomonas aeruginosa*. This facet of the study aligns with the growing concerns about biofilm-associated antibiotic resistance and the multifaceted role of biofilm formation in the pathogenicity of *P.*

aeruginosa as a biofilm-forming, multidrug resistant bacterial strain for which alternative antimicrobial therapies are urgently needed.

Crystal violet biofilm formation assays were performed on the PA01 wild-type, PA01-425 (ΔPA5189), and PA01-428 (PA5189 overexpression) strains, cultivated in different growth media: LB Miller, Tryptic Soy (TS), and cation-adjusted Mueller-Hinton broth (CAMHB). Intriguingly, while the PA01 wild-type and the PA01-425 knockout strain exhibited comparable levels of biofilm formation across all tested media, PA01-428 displayed a markedly variable biofilm profile: an almost twofold increase in TS broth and a more than twofold decrease in CAMHB, relative to the wild-type and ΔPA5189 strains. Consistently, all strains showed similar biofilm levels in LB broth (refer to Figure 5 for detailed visualization).

This differential biofilm formation pattern, particularly in the PA01-428 strain, suggests that the upregulation of PA5189 significantly alters biofilm dynamics, contingent on the specific nutritional composition of the environment. The observed increase in biofilm formation in TS broth and decrease in CAMHB in the PA01-428 strain may be attributed to variations in nutrient composition among these media. LB miller broth, for example, is comprised of 5 g/L yeast extract, 10 g/L peptone, and 10 g/L NaCl, contrasting with the richer nitrogen content and decreased salt content relative to LB Miller as well as the presence of a glucose source in TS broth and CAMHB.

These observations imply that, in an overexpression context, PA5189's influence on biofilm formation is significantly modulated by the availability of specific nutrients, particularly nitrogen and glucose, as well as salt concentration. The results also suggest that upregulation of PA5189 causes significantly decreased biofilm formation in the presence of relatively low salt content, relatively high nitrogen content, and in the presence of glucose. Meanwhile, in the presence of high salt content, relatively lower nitrogen content, and in the absence of glucose, differential expression of PA5189 does not impact biofilm formation.

These findings thus suggest that upregulation of PA5189 significantly impacts biofilm formation under various nutrient conditions and are consistent with previous research linking PA5189 to *BsrA,* which has been found to directly regulate genes involved biofilm formation, glucose metabolism, and nitrogen metabolism [44].

Conclusion

In an age of antibiotic resistance, the development of alternatives and adjuncts to standard antimicrobial therapies is underscored by a need to understand the genetic networks underlying cellular processes involved in virulence. In this study, we utilized a workflow for the generation and characterization of PA5189 deletion mutants in *P. aeruginosa* to further characterize its impact in virulence processes such as antibiotic susceptibility and biofilm formation.

In the broader context of the increasing threat of antibiotic and multidrug resistance, especially in biofilm-forming bacterial species, the findings from this study highlight the complexity of genetic networks in *P. aeruginosa* that contribute to its notorious resilience against antimicrobial therapies. Understanding the nuances of such regulatory networks, especially the roles of lesser-known genes like PA5189, is pivotal in developing targeted antimicrobial strategies and combating the pervasive challenge of drug-resistant infections. This nuanced understanding aligns with previous research that connects PA5189 to *BsrA*, a gene implicated in the direct regulation of pathways involved in biofilm formation, glucose metabolism, and nitrogen metabolism [44]. In an era where the pervasiveness of antibiotic and multidrug resistance is a major global health concern, the elucidation of such regulatory mechanisms becomes crucial. Understanding how genetic factors like PA5189 influence biofilm formation under various nutrient conditions can offer insights into the complex interplay between bacterial growth environments, genetic regulation, and the consequent impact on antibiotic resistance.

In summary, our findings illuminate the significant yet variable impact of PA5189 expression on drug sensitivity and biofilm formation in *P. aeruginosa*. This variability, dictated largely by the expression context and nutritional environment, underscores the adaptability of *P. aeruginosa* and the importance of considering environmental factors when studying bacterial resistance mechanisms. We propose that future research be conducted investigating the role of nutrient composition in biofilm synthesis, possibly focusing on the impact of using minimal media in assays investigating the biofilm-forming capacities PA5189 and other transcription factor perturbation mutants. Our work also offers avenues for future investigations into novel therapeutic interventions, given that our data supports previous findings implicating PA5189 in a complex transcriptional regulatory network mediating carbon and nitrogen metabolism, drug sensitivity (possibly by way of modulating drug entry and export mechanisms), quorum sensing, and biofilm synthesis. As such, these insights contribute to a broader understanding of the genetic and environmental factors that govern biofilm formation and antibiotic resistance in *Pseudomonas aeruginosa*, offering potential avenues for developing targeted strategies to combat persistent infections and drug resistance in clinical and agricultural settings.

References

1. Jones, R.N., (1990). Important and Emerging b-Lactamase-mediate Resistances in Hospital-based Pathogens: The Amp C Enzymes. *Diagn. Microbiol. Infect. Dis., 31*:461-6.

2. Poole, K., (2002). Outer Membranes and Efflux: The Path to Multidrug Resistance in Gram-Negative Bacteria. *Curr. Pharm. Biotech.*, *3*(2):77-98.

3. Zhanel, G.G., et al., (2004). Role of efflux mechanisms on fluoroquinolone resistance in *Streptococcuspneumonia* and *Pseudomonas aeruginosa*. *Int. J. Antimic. Agents, 24*(6):529-35.

4. Slama, T.G., (2008). Gram-negative antibiotic resistance: there is a price to pay. *Crit. Care, I2*(Suppl):4.

5. Urban-Chmiel, R., et al., (2022). Antibiotic Resistance in Bacteria—A Review. *Antibiotics, 11*(8).

6. Zhu, Y., et al., (2022). Clinical Perspective of Antimicrobial Resistance in Bacteria. *Infect. Drug Resist., 15*:735-46.

7. Chang, H., et al., (2015). Origin and Proliferation of Multiple-Drug Resistance in Bacterial Pathogens. *Microbiol. Mol. Biol. Rev., 79*(1):101-16.

8. Catalano, A., et al., (2022). Multidrug Resistance (MDR): A Widespread Phenomenon in Pharmacological Therapies. *Molecules, 27*(3):616.

9. Hoang, T.T., et al., (1998). A broad-host-range Flp-FRT recombination system for site-specific excision of chromosomally-located DNA sequences: application for isolation of unmarked *Pseudomonas aeruginosa* mutants. *Gene, 212*(1):77-86.

10. Stover, C.K., et al, (2000). Complete genome sequence of *Pseudomonas aeruginosa* PA01, an opportunistic pathogen. *Nature, 406,* (6799):959-64.s

11. Schweizer, H.D., (1993). Small broad-host-range gentamycin resistance gene cassettes for site-specific insertion and deletion mutagenesis. *Biotechniques, 15*(5):831-4.

12. Ciofu, O, et al., (2017). Antibiotic treatment of biofilm infections. *J. Path. Microbiol. Immun., 125*(4):304-19.

13. Römling, U., and Balsalobre, C., (2012). Biofilm infections, their resilience to therapy and innovative treatment strategies. *J. Int. Med., 272*(6):541-61.

14. Gebreyohannes, G., et al., (2019). Challenges of intervention, treatment, and antibiotic resistance of biofilm-forming organisms. *Heliyon, 5*(8):e02192.

15. Green, M.R., Sambrook, J., and Cold Spring Harbor Laboratory, (2012). Molecular cloning: a laboratory manual. Cold Spring Harbor, N.Y: *Cold Spring Harbor Laboratory Press*.

16. Diggle, S.P., et al., (2006). The galactophilic lectin, LecA, contributes to biofilm development in *Pseudomonas aeruginosa*.

17. del Pozo, J.L., and Patel, R., (2007). The challenge of treating biofilm-associated bacterial infections. *Clin. Pharmacol. Ther., 82*(2):204-9.

18. Wu, H., et al., (2014). Strategies for combating bacterial biofilm infections. *Int. J. Oral Sci., 7*:1-7.

19. Jo, J., et al., (2022). Gradients and consequences of heterogeneity in biofilms. *Nature Rev. Microbiol.,* 20:593-607.

20. Reyes, L.M., et al., (2020). Enhancing bacterial survival through phenotypic heterogeneity. *PLoS Pathog., 16*(5):e1008439.

21. Schiessl, K.T., et al., (2019). Phenazine production promotes antibiotic tolerance and metabolic heterogeneity in *Pseudomonas aeruginosa* biofilms. *Nature Comm., 10*:672.

22. Slonov, R.V., and Steinberg, D., (2022). Targeting the holy triangle of quorum sensing, biofilm formation, and antibiotic resistance in pathogenic bacteria. *Microorganisms, 10*(6):1239.

23. Brindhadevi, K., et al., (2020). Biofilm and quorum sensing mediated pathogenicity in *Pseudomonas aeruginosa, 96*:59-47.

24. Stewart, P.S., et al., (2008). Physiological heterogeneity in biofilms. *Nature Rev. Microbiol., 6*:199-210.

25. Muhammad, M.H., et al., (2020). Beyond risk: Bacterial biofilms and their regulating approaches. *Front. Microbiol., 11*(928).

26. Pelling, H., et al, (2019). Bacterial biofilm formation on indwelling urethral catheters. *Lett. Appl. Microbiol., 68*(4):277-93.

27. Koley, D., et al., (2011). Discovery of a biofilm electrocline using real-time 3D metabolite analysis. *Proc. Natl. Acad. Sci. U. S. A., 108*(50):19996-20001.

28. Huang, W., and Wilks, A., (2017). A rapid seamless method for gene knockout in *Pseudomonas aeruginosa*. *BMC Microbiol., 17*(199).

29. Scott, Z.W., (2019). Characterization of the role of PA5189 of *Pseudomonas aeruginosa* in resistance to an antimicrobial peptide. [Master's thesis, University of Nebraska at Omaha].

30. Hou, J., et al., (2023). Global trend of antimicrobial resistance in common bacterial pathogens in response to antibiotic consumption. *J. Hazard. Materials, 442*:130042.

31. Murray, C.J.L, et al. (2022). Global burden of bacterial antimicrobial resistance in 2019: a systematic analysis. *Lancet, 399*(10325):629-55.

32. Michaelis, C, and Grohmann, E., (2023). Horizontal gene transfer of antibiotic resistance genes in biofilms. *Antibiotics, 12*(2):328.

33. Laxminarayan, R., et al., (2016). Access to effective antimicrobials: a worldwide challenge. *Lancet, 387*(10014):168-75.

34. Podolsky, S.H., (2018). The evolving response to antibiotic resistance (1945-2018), *Palgrave Communications, 4*(124).

35. Jonas, O.B., et al., (2017). Drug-resistant infections: a threat to our economic future (Vol. 2) : final report (English). HNP/Agriculture Global Antimicrobial Resistance Initiative Washington, D.C.*: World Bank Group*.

36. Biondo, C., (2023). Bacterial antibiotic resistance: the most critical pathogens. *Pathogens, 12*(1):116.

37. Streeter, K., and Katouli, M., (2016). *Pseudomonas aeruginosa*: A review of their pathogenesis and prevalence in clinical settings and the environment. *Infect. Epidemiol. Med., 2*(1):25-32.

38. Reynolds, D., and Kollef, M., (2021). The epidemiology and pathogenesis and treatment of *Pseudomonas aeruginosa* infections: An update. *Drugs, 81*(18):2117-31.

39. Mulani, M.S, et al., (2019). Emerging strategies to combat ESKAPE pathogens in the era of antimicrobial resistance: A review. *Front. Microbiol., 10*:539.

40. Thi, M.T.T., et al., (2020). *Pseudomonas aeruginosa* biofilms. *Int. J. Mol. Sci., 21*(22):8671.

41. Maurice, N.M., et al., (2018). *Pseudomonas aeruginosa* biofilms: Host response and clinical implications in lung infections. *Am. J. Respir. Cell. Mol. Biol., 58*(4):428-39.

42. Wang, T., et al., (2021). An atlas of the binding specificities of transcription factors in *Pseudomonas aeruginosa* directs prediction of novel regulators in virulence. *eLife, 10:*e61885.

43. Shao, X., et al., (2022). The transcriptional regulators of virulence for *Pseudomonas aeruginosa*: Therapeutic opportunity and preventative potential of its clinical infections. *Genes and Diseases, 10*(5):2049-63.

44. Modrzejewska, M., et al., (2021). The LysR-type transcription regulator BsrA (PA2121) controls vital metabolic pathways in *Pseudomonas aeruginosa*. *mSystems, 6*:e00015-21.

45. Vologodskii, A.V., et al., (1998). Sedimentation and electrophoretic migration of DNA knots and catenanes. *J. Mol. Biol., 278*(1):1-3.

46. Vogelstein, B., and Gillespie, D., (1979). Preparative and analytical purification or DNA from agarose. *Proc. Natl. Acad. Sci. USA, 76*:615-19.

47. Coffey, B.M., and Anderson, G.G., (2014). Biofilm formation in the 96-well microtiter plate. In: Filloux, A., Ramos, J.L. (eds) Pseudomonas Methods and Protocols. *Methods in Molecular Biology, 1149*:631-41. Humana, New York, NY.

48. Hashizume, T., et al., (1984). Studies on the mechanism of action of imipenem (n-formimidoylthienamycin) *in vitro*: Binding to the penicillin-binding proteins (PBPs) in *Escherichia coli* and *Pseudomonas aeruginosa*, and inhibition of enzyme activities due to the PBPs in *E. coli*. *J. Antibiot., 37*(4):394-400.

49. Sanders, C. C., (1988). Ciprofloxacin: In vitro activity, mechanism of action, and resistance. *Rev. Infect. Dis., 10*(3):516-27.